Perovskites

Deutsche Ausgabe: DOI: 10.1002/ange.201503153
Internationale Ausgabe: DOI: 10.1002/anie.201503153

The Role of Oxygen in the Degradation of Methylammonium Lead Trihalide Perovskite Photoactive Layers**

*Nicholas Aristidou, Irene Sanchez-Molina, Thana Chotchuangchutchaval, Michael Brown, Luis Martinez, Thomas Rath, and Saif A. Haque**

Abstract: *In this paper we report on the influence of light and oxygen on the stability of $CH_3NH_3PbI_3$ perovskite-based photoactive layers. When exposed to both light and dry air the mp-Al_2O_3/$CH_3NH_3PbI_3$ photoactive layers rapidly decompose yielding methylamine, PbI_2, and I_2 as products. We show that this degradation is initiated by the reaction of superoxide (O_2^-) with the methylammonium moiety of the perovskite absorber. Fluorescent molecular probe studies indicate that the O_2^- species is generated by the reaction of photoexcited electrons in the perovskite and molecular oxygen. We show that the yield of O_2^- generation is significantly reduced when the mp-Al_2O_3 film is replaced with an mp-TiO_2 electron extraction and transport layer. The present findings suggest that replacing the methylammonium component in $CH_3NH_3PbI_3$ to a species without acid protons could improve tolerance to oxygen and enhance stability.*

Over the last few years, organic lead halide perovskites have aroused enormous interest with respect to their application in low-cost, solution-processable photovoltaics. A wide range of device architectures employing such perovskite absorbers have been reported so far, with efficiencies approaching 20%.[1–4] In spite of this tremendous progress, a number of key issues must be overcome before wide-spread commercialization is possible, mainly, those associated with toxicity of lead, understanding phase behavior,[5] and long-term material stability. Regarding the latter, UV irradiation[6] and water, are well known to affect the stability of methylammonium lead triiodide ($CH_3NH_3PbI_3$, $MAPbI_3$, MAPI).[1,7,8] Recently, a few mechanistic studies on the action of water on $CH_3NH_3PbI_3$ have been reported, identifying lead(II) iodide as one of the final products, although different degradation pathways were proposed.[9,10] Moreover, we have recently reported that decomposition of $CH_3NH_3PbI_3$ can also be triggered by the combination of molecular oxygen and light.[10] More specifically, in our previous work we employed transient absorption spectroscopy to monitor the yield of long-lived charge separation in mesoporous TiO_2/$CH_3NH_3PbI_3$/spiro-OMeTAD and Al_2O_3/$CH_3NH_3PbI_3$/spiro-OMeTAD photoactive layers before and after exposure to light and oxygen. After the ageing process, the mesoporous Al_2O_3-based samples showed a rapid and substantial drop in the yield of long-lived charge separation. We attributed this drop in yield to degradation of the $CH_3NH_3PbI_3$ absorber resulting from a reaction between oxygen and the photoexcited electrons in $CH_3NH_3PbI_3$. Moreover, this degradation pathway was apparently hindered in the mesoporous TiO_2-based samples; here electron injection from the photoexcited state of $CH_3NH_3PbI_3$ precludes this parasitic decomposition reaction. In this paper, we build on our previous work and report on the mechanism of this photodegradation reaction. Specifically, we show that the combined action of light and molecular oxygen on $CH_3NH_3PbI_3$ photoactive layers results in the decomposition of the perovskite leading to the formation of PbI_2, I_2, and methylamine. Importantly, we show that this photodegradation reaction is triggered by the action of a reactive oxygen species (superoxide; O_2^-) on the organic (i.e., methylammonium) component of the $CH_3NH_3PbI_3$ perovskite absorber. The present findings indicate that the identification of alternative cations to methylammonium ($CH_3NH_3^+$) may be of crucial importance to the design of environmentally stable organometal trihalide perovskite photovoltaic devices.

To investigate whether superoxide generation contributes to the degradation of $CH_3NH_3PbI_3$ photoactive layers and leads to their reduced photochemical stability under illumination in a moisture-free atmosphere, a molecular fluorescent probe, hydroethidine (HE) was employed. This compound is known to show a characteristic increase in emission at 610 nm upon exposure to the superoxide radical anion.[12] $CH_3NH_3PbI_3$ films were fabricated onto two glass substrates coated either with mp-TiO_2 or mp-Al_2O_3. The resulting mp-TiO_2/$CH_3NH_3PbI_3$ and mp-Al_2O_3/$CH_3NH_3PbI_3$ films were then immersed into a 0.317 μM solution of the HE probe in dry toluene. The photodegradation conditions consisted of ageing the samples under continuous illumination from a tungsten halogen lamp and dry air flow (21% oxygen content). In the current experiment, the fluorescence emission of the HE probe was monitored at regular time intervals over the course of one hour with the mp-TiO_2/$CH_3NH_3PbI_3$ and mp-Al_2O_3/$CH_3NH_3PbI_3$ films exposed to light and dry air. Figure 1a shows the emission characteristics of HE (fluorescence intensity versus wavelength) as a function of ageing time for both mp-TiO_2/$CH_3NH_3PbI_3$ and mp-Al_2O_3/

[*] N. Aristidou, Dr. I. Sanchez-Molina, T. Chotchuangchutchaval, Dr. M. Brown, Dr. L. Martinez, Dr. T. Rath, Prof. S. A. Haque
Department of Chemistry, Imperial College London
South Kensington Campus, London SW7 2AZ (United Kingdom)
E-mail: s.a.haque@imperial.ac.uk

[**] S.A.H. acknowledges financial support from the Engineering and Physical Sciences Research Council (EPSRC) through EP/H040218/2 and EP/K010298/1 projects. S.A.H. acknowledges financial support from the European Community's Seventh Framework Programme (Nanomatcell, grant agreement number 308997). T.R. acknowledges financial support from the Austrian Science Fund (FWF) under the grant number J3515-N20.

Supporting information for this article is available on the WWW under http://dx.doi.org/10.1002/anie.201503153.

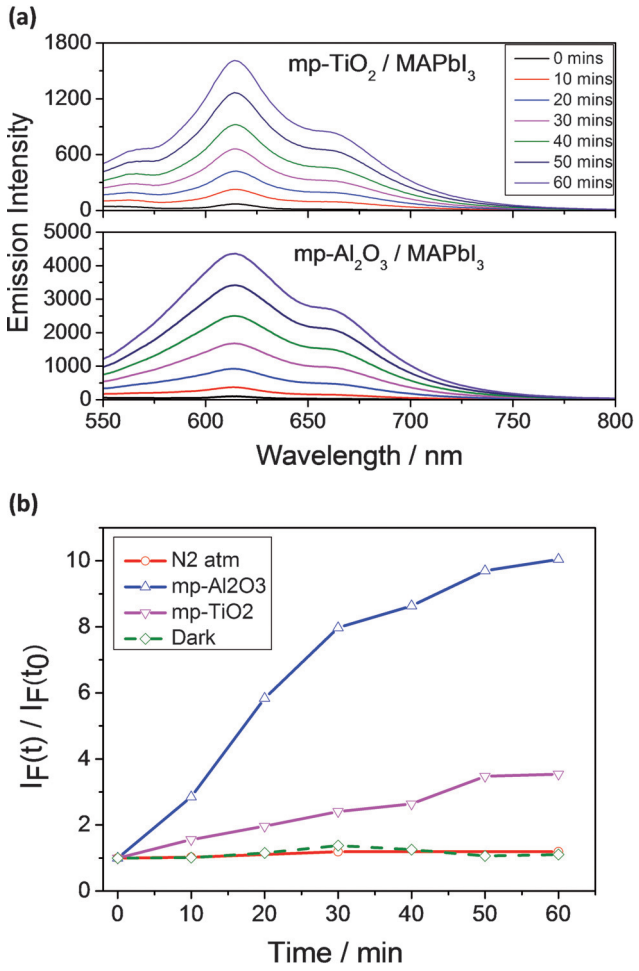

Figure 1. a) Raw emission data collected from the probe solution, highlighting the increasing intensity observed with ageing under illumination and dry air flux. b) Normalized fluorescence intensity at 610 nm of the superoxide probe solution, with excitation at 520 nm. $I_F(t)$ is the fluorescence intensity maximum at time t, whilst $I_F(t_0)$ is the background fluorescence intensity of the probe at $t=0$. The ratio $I_F(t)/I_F(t_0)$ is a measure of the yield of superoxide generation.

$CH_3NH_3PbI_3$. The rate of increase in emission ($[I_F(t)/[I_F(t_0)]$ at 610 nm versus ageing time), and therefore superoxide generation is shown in Figure 1b. Control measurements performed in the absence of light (green curve, Figure 1b) showed no increase in HE emission at 610 nm, indicating that the process is photoinduced. Similarly, when the dry air stream was replaced with nitrogen and illumination was introduced, there was no detectable increase in fluorescence intensity (red curve, Figure 1b). In contrast, when the mp-TiO_2/$CH_3NH_3PbI_3$ and mp-Al_2O_3/$CH_3NH_3PbI_3$ samples were exposed to both dry air and light, the expected increase of fluorescence of the probe was observed, which is consistent with the presence of superoxide in the solution. However, it is apparent from the data presented in Figure 1b that a higher yield of superoxide generation is observed in the mp-Al_2O_3/$CH_3NH_3PbI_3$ film as compared to the analogous mp-TiO_2/$CH_3NH_3PbI_3$ sample. The next question that arises relates to why the mp-Al_2O_3/$CH_3NH_3PbI_3$ film exhibits a greater yield of superoxide generation than the mp-TiO_2/$CH_3NH_3PbI_3$ sample. A key difference between using mesoporous TiO_2 and Al_2O_3 films is that the TiO_2 film can accept an electron from the photoexcited perovskite, due to a favorable energy offset at the heterojunction,[13] as shown in Figure 2. This, in

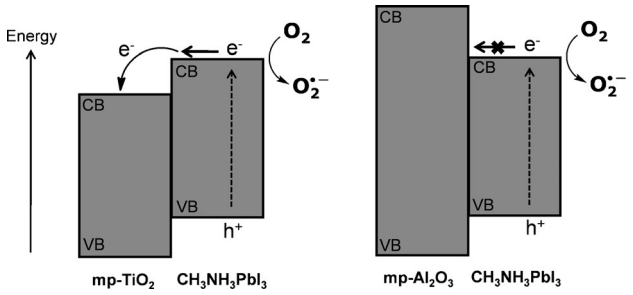

Figure 2. Schematic model showing the electron transfer of the photoexcited electrons in the $MAPbI_3$ layers to oxygen resulting in the formation of superoxide. A higher yield of superoxide generation is seen in the $Al_2O_3/MAPbI_3$ system as compared to the $TiO_2/MAPbI_3$ system. In the $Al_2O_3/MAPbI_3$ system, the electrons remain on the perovskite and can react with oxygen to form superoxide. If the perovskite is prepared on mp-TiO_2, the photoexcited electrons can be injected into the mesoporous TiO_2. In the $TiO_2/MAPbI_3$ system electron transfer from the perovskite to the mp-TiO_2 can successfully compete with electron transfer from the perovskite to oxygen resulting in a reduced yield of superoxide production.

turn, would reduce the number of photoexcited electrons in the perovskite available for electron transfer to oxygen, thereby reducing the yield of superoxide generation, which is consistent with the data presented in Figure 1. We hypothesize that the relatively low yield of superoxide generation in the mp-TiO_2/$CH_3NH_3PbI_3$ film (as compared to the Al_2O_3-based sample) is most likely due to the presence of a $CH_3NH_3PbI_3$ overlayer as revealed by scanning electron microscopy (SEM) studies. Support for this assertion comes from cross-sectional scanning electron microscopy studies which revealed the presence of an approximately 50 nm thick overlayer of perovskite in both mp-Al_2O_3/$CH_3NH_3PbI_3$ and mp-TiO_2/$CH_3NH_3PbI_3$ films (see the Supporting Information, Figure S1). As such, the reduced rate of production of superoxide in the TiO_2-based samples compared to that of the Al_2O_3-based films could thus arise as a consequence of the photoinduced electron transfer process from $CH_3NH_3PbI_3$ to the TiO_2 layer being in direct competition with the reaction of the photogenerated electrons with oxygen. Furthermore, it is pertinent to note that our observation of increased superoxide production in Al_2O_3 samples is in good agreement with our previous work showing a rapid and profound degradation in the yield of photoinduced charge separation in mp-Al_2O_3/$CH_3NH_3PbI_3$/spiro-OMeTAD films upon exposure to light and dry air.[11] Moreover, the present findings suggest that the yield of superoxide generation can be significantly reduced by ensuring that the photogenerated electrons in the perovskite are rapidly extracted before they can react with oxygen.

We now consider the compositional changes in the $CH_3NH_3PbI_3$ perovskite film resulting from the ageing process. To elucidate the products of the degradation that occurs as a result of the combination of light and dry air, we

immersed the substrates in dry toluene under a constant flow of dry oxygen and illumination, thus excluding moisture. Similar to the HE probe experiments, mp-Al_2O_3-based films were immersed in dry toluene and then a constant flow of dry oxygen and illumination were used to create the controlled degradation conditions. It was noted that after 72 h exposure to both light and oxygen the $CH_3NH_3PbI_3$ perovskite films changed color from dark brown to yellow and the toluene solution turned light pink, most likely due to the formation of iodine. UV/Vis spectroscopy was used to monitor the evolution of iodine in the solution (Figure 3a). The change in the absorption spectra is consistent with the production of iodine, as the detected absorption spectrum resembles the absorption of iodine.[14] The addition of sodium thiosulfate, which can reduce iodine to iodide, turned the solution colorless, which further supports the identification of the product as iodine.

To further analyze the compositional change in the aged films, scanning electron microscopy energy-dispersive X-ray spectroscopy (SEM-EDX) measurements were performed. EDX analysis showed the Pb/I ratio to deplete from 1:3 to 1:2 in the fresh and degraded samples respectively, as illustrated in Figure 3b.

An X-ray diffraction analysis of the samples shows the characteristic peaks of methylammonium lead iodide in the fresh sample (Figure 4).[15,16] These peaks are largely diminished in the degraded sample and distinct additional peaks stemming from PbI_2 are detected. The formation of PbI_2 was additionally confirmed by Raman spectroscopy, which clearly shows the characteristic peaks of PbI_2 that coincide with a PbI_2 reference sample (Figure S2).

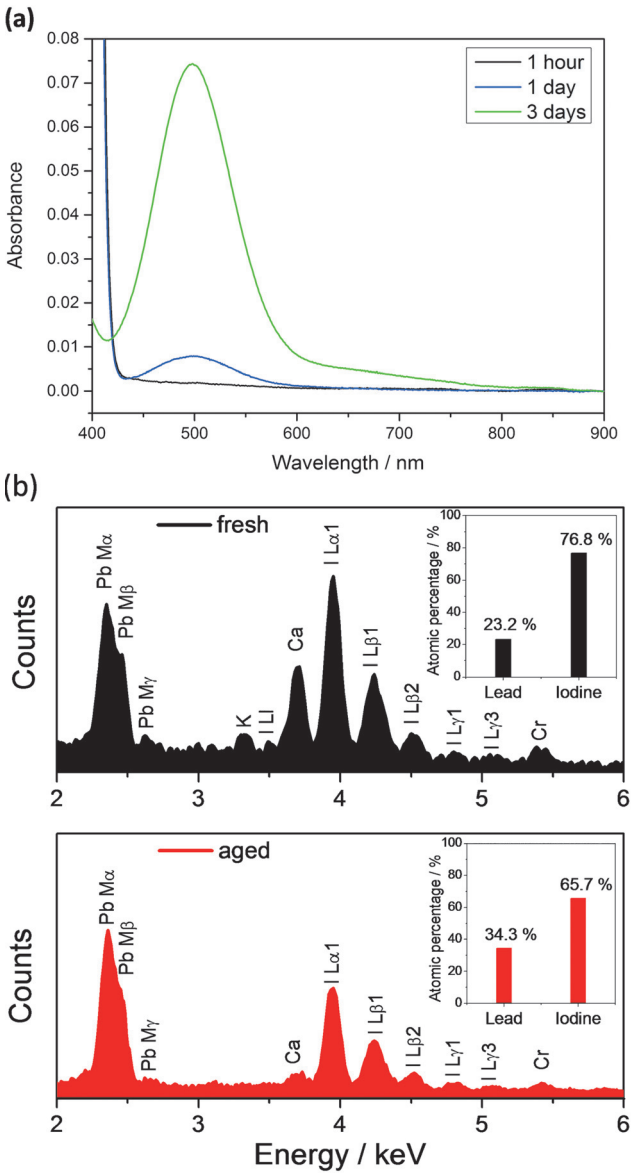

Figure 3. a) UV/Vis spectra showing the production of iodine over a 72-hour time period, during which the mp-Al_2O_3/MAPI films were continuously subjected to the degradation conditions. b) SEM-EDX spectra and elemental composition analysis showing that on ageing (for 72 h) the molar ratio of Pb/I in the sample changes from 1:3 to 1:2. Peaks in the spectra not assigned to Pb or I stem from the glass substrate or the chromium coating of the samples to prevent charging during the SEM-EDX analysis.

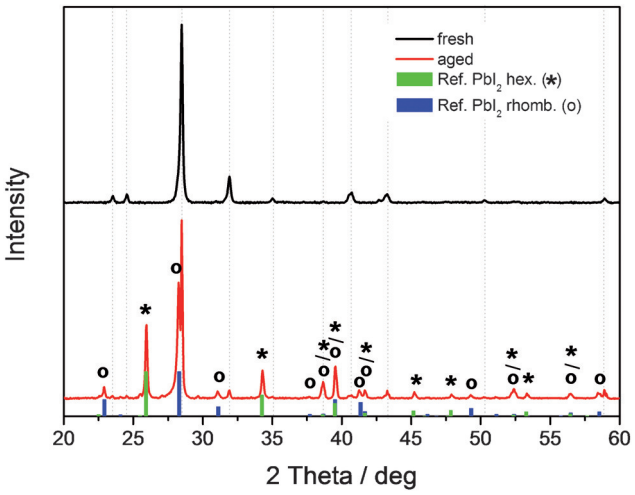

Figure 4. X-ray diffraction patterns of a fresh and an aged (for 72 h) sample showing the formation of PbI_2 as the result of degradation in a moisture-free environment. Dotted vertical lines in the graph indicate the peak positions of methylammonium lead iodide according to literature data.[15,16] The additional peaks in the degraded sample can be assigned to PbI_2 (reference patterns: PDF 01-080-1000 for hexagonal and PDF 01-073-1753 for rhombohedral PbI_2).

Having identified two of the degradation products, the next question that arises relates to how the superoxide species causes degradation of the perovskite. One possibility is that the superoxide reacts with the organic component of the perovskite (i.e. methylammonium cation). To test this hypothesis and to better understand the degradation mechanism we investigated whether the methylammonium cations are undergoing any transformation. For this purpose, a model reaction was set up and NMR was employed to monitor the transformation. The model reaction consisted of a sample of methyl ammonium iodide (MAI) dissolved in dry ethanol, to which potassium superoxide (KO_2) was added. The sample was then transferred to an NMR tube to which some

deuterated acetone was added for calibration of the spectrum. The reaction proceeded with a color change, from colorless to orange. Proton NMR spectra of the sample and of a control containing only methylammonium iodide are shown in Figure 5. Both the signal for the NH_3^+ and the methyl group

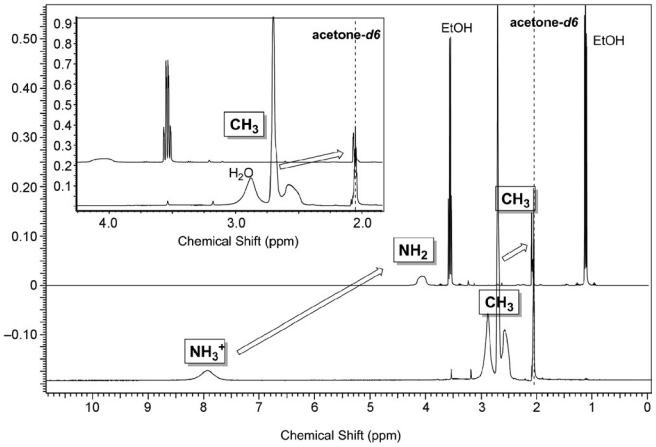

Figure 5. NMR Spectra of a reference sample containing methylammonium iodide (bottom) and the resulting spectra after addition of potassium superoxide. Inset shows an expansion of the methyl signal.

protons shift up-field upon addition of potassium superoxide, which is consistent with the deprotonation of the ammonium group to form methylamine ($MeNH_2$). The presence of iodine in the sample was again determined by the addition of sodium thiosulfate, which turned the solution from orange to colorless. The pH of the solution was also estimated with pH-paper to be around 10. This could be accounted for by the potential formation of KOH due to the potassium salt being used in the model reaction. It is therefore plausible that water can be formed in the oxygen- and light-assisted degradation of $CH_3NH_3PbI_3$.

Herein we have shown that the degradation of the mp-Al_2O_3/$CH_3NH_3PbI_3$ sample in a moisture-free environment can be accounted for by the generation of superoxide through electron transfer from the photoexcited perovskite phase to molecular oxygen. The present findings suggest that the superoxide acts to break down the perovskite by first deprotonating the methylammonium cation as shown by NMR spectroscopy. Moreover, the deprotonation of the methylammonium cation ultimately leads to the formation of PbI_2, as confirmed by XRD and Raman spectroscopy, and iodine, detected by UV/Vis spectroscopy and confirmed by addition of sodium thiosulfate. Based on these observations we propose a possible reaction scheme for the degradation (Figure 6). It is pertinent that water is expected to be another by-product of decomposition as discussed above. The resulting water could then participate in further degradation pathways, perhaps similar to the ones reported in the literature, in which water would now act as an active species in the degradation or act to hydrate the perovskite.[9,10] The overall effect after a first action of superoxide on the perovskite will be an increase of the decomposition rate, because, even if the $CH_3NH_3PbI_3$ is carefully encapsulated in

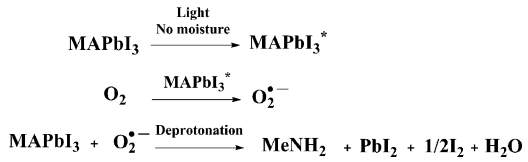

Figure 6. Potential route for degradation caused by superoxide as predicted from the obtained data reported herein. Optical excitation of $MAPbI_3$ results in the formation of $MAPbI_3$*. $MAPbI_3$* is s species that carries both photoinduced electrons and holes. Superoxide is generated through electron transfer from $MAPbI_3$* to O_2. The resulting superoxide attacks the perovskite absorber leading to the formation of methylamine ($MeNH_2$), lead iodide, iodine, and water as degradation products.

a water-free environment, degradation can be triggered by the presence of oxygen and light. The data presented in this paper and reported in our previous work[11] show that the $CH_3NH_3PbI_3$ films rapidly degrade (e.g., on a timescale of a few hours to days) when exposed to both light and oxygen. As such, this light- and oxygen-induced degradation pathway could have a significant impact on perovskite solar cell device performance and long-term device stability. It is therefore crucial to ensure that $CH_3NH_3PbI_3$ perovskite layers, when incorporated in photovoltaic devices, are isolated from both water and oxygen. The data presented in this paper suggests that the superoxide-mediated degradation pathway can be significantly reduced or even prevented by ensuring that the photogenerated electrons on the perovskite are extracted before they can react with oxygen to form superoxide. Herein, we have shown that the implementation of a mesoporous electron-extracting layer (e.g., mp-TiO_2) can facilitate the deactivation of the electron transfer process to oxygen, resulting in reduced superoxide generation. Obtaining more efficient electron extraction should lead to enhanced stability in ambient and moisture-free environments. Alternatively material design aimed at replacing the methylammonium cation to a species without acid protons could improve stability and may alleviate the need for oxygen barriers.

Experimental Methods

Materials: All chemicals were purchased from Sigma–Aldrich and used as received, except TiO_2 nanoparticles from Dyesol and methylammonium iodide, which was synthesized in the lab. Anhydrous toluene was filtered through silica gel prior to use.

Synthesis of methylammonium iodide: Methylamine solution (33 wt%) in ethanol (6.2 mL, 0.046 mol) was cooled down in an ice bath. Hydroiodic acid solution (55 wt%) in water (10 mL, 0.073 mol) was then added dropwise under vigorous stirring. The reaction was stirred for 1 h at 0°C. The product precipitated from the solution as a white-yellowish solid. Ethanol (5 mL) was added to ensure full precipitation of the solid, which was filtered and washed with cold ethanol. Recrystallization of the product in chloroform afforded the pure compound as white crystalline solid (6.4 g, 87%).

Film Fabrication: All films were deposited onto clean glass substrates with a size of ca. 1 × 1 cm. The glass substrates were washed sequentially in acetone, deionized water and isopropanol (IPA) under sonication for 10 min during each washing cycle. A Laurell Technologies WS-650MZ-23NPP Spin Coater was used to fabricate the films. A 1M solution of $CH_3NH_3PbI_3$ was formed by adding PbI_2 in

a 1:1 molar ratio with methylammonium iodide in a solvent mixture of 4:1 gamma-butyrolactone (GBL) to DMSO. This solution was then spin-coated onto the substrates using a consecutive two-step spin program under a nitrogen atmosphere in a glovebox. The first spinning cycle is performed at 1000 rpm for 10 s followed by 5000 rpm for 20 s, as reported by Jeon et al.[17] During the second phase, the substrate was treated with toluene ($\approx$350 μL) drop-casting. The films were then annealed at 100 °C for 10 min. The perovskite layers were deposited onto mesoporous Al_2O_3 and mesoporous TiO_2 films prepared as follows:

a) Mesoporous Al_2O_3 layers were fabricated on cleaned glass substrates by spin coating (4500 rpm for 45 s) an Al_2O_3 dispersion prepared in a 2:1 vol. ratio of Al_2O_3 (< 50 nm particle size in IPA solution) and IPA. After spin coating, the films were placed on a hotplate at 150 °C for 30 min.

b) Mesoporous TiO_2-based films were fabricated using a paste of 20 nm TiO_2 nanoparticles in a 1:5 weight ratio with dry ethanol. This was spin-coated onto glass substrates at 6000 rpm for 30 s. Once spun, the films were sintered at 450 °C for 1 h in a furnace.

Probe Testing: A stock solution (31.7 μM) of the hydroethidine (HE) probe was prepared by dissolving 10 mg HE in 10 mL of dry toluene; sonication was used to facilitate miscibility. Films were then added to 10 mL of 0.317 μM solution created from the stock solution. Photoluminescence spectra were recorded using an excitation wavelength of 520 nm and a slit width of 10 mm on a Horiba Jobin–Yvon Fluorolog-3 spectrofluorometer. In the experiments with oxygen involved, dry oxygen was bubbled through the toluene. For the control using N_2, a Schlenk line was used to keep a continuous flow of nitrogen through the system.

Ageing Conditions: Films were submerged in 10 mL dry toluene. Toluene (Sigma–Aldrich 99.8 %) was dried over molecular sieves, with a pore size of ca. 3 Å. Dry air was gassed through for the duration of the degradation. Illumination was provided by a tungsten halogen lamp of approximately 1.5 mW cm^{-2} power.

Superoxide Model Reaction: Potassium superoxide and methylammonium iodide were dissolved in a 1:1 molar ratio in dry ethanol. The reaction resulted in a color change from colorless to orange.

Characterization: ^{1}H NMR spectra were recorded on a 400 MHz Bruker spectrometer using TopSpin software. UV/Vis spectra were acquired on a PerkinElmer UV/VIS Spectrometer Lambda 25. X-ray diffraction patterns were measured on a PANalytical X'Pert Pro MRD diffractometer using Ni filtered Cu K_α radiation at 40 kV and 40 mA. SEM-EDX measurements were carried out on a JEOL 6400 scanning electron microscope operated at 20 kV.

Keywords: methylammonium lead triiodide · perovskites · solar cells · spectroscopy · stability

How to cite: *Angew. Chem. Int. Ed.* **2015**, *54*, 8208–8212
Angew. Chem. **2015**, *127*, 8326–8330

[1] J. Burschka, N. Pellet, S.-J. Moon, R. Humphry-Baker, P. Gao, M. K. Nazeeruddin, M. Graetzel, *Nature* **2013**, *499*, 316–319.
[2] D. Bi, S.-J. Moon, L. Haggman, G. Boschloo, L. Yang, E. M. J. Johansson, M. K. Nazeeruddin, M. Graetzel, A. Hagfeldt, *RSC Adv.* **2013**, *3*, 18762–18766.
[3] M. M. Lee, J. Teuscher, T. Miyasaka, T. N. Murakami, H. J. Snaith, *Science* **2012**, *338*, 643–647.
[4] O. Malinkiewicz, A. Yella, Y. H. Lee, G. Minguez Espallargas, M. Graetzel, M. K. Nazeeruddin, H. J. Bolink, *Nat. Photonics* **2014**, *8*, 128–132.
[5] T.-B. Song, Q. Chen, H. Zhou, S. Luo, Y. Yang, J. You, Y. Yang, *Nano Energy* **2015**, *12*, 494–500.
[6] T. Leijtens, G. E. Eperon, S. Pathak, A. Abate, M. M. Lee, H. J. Snaith, *Nat. Commun.* **2013**, *4*, 2885.
[7] H. P. Zhou, Q. Chen, G. Li, S. Luo, T. B. Song, H. S. Duan, Z. R. Hong, J. B. You, Y. S. Liu, Y. Yang, *Science* **2014**, *345*, 542–546.
[8] J. A. Christians, P. A. Miranda Herrera, P. V. Kamat, *J. Am. Chem. Soc.* **2015**, *137*, 1530–1538.
[9] G. Niu, W. Li, F. Meng, L. Wang, H. Dong, Y. Qiu, *J. Mater. Chem. A* **2014**, *2*, 705–710.
[10] J. Yang, B. D. Siempelkamp, D. Liu, T. L. Kelly, *ACS Nano* **2015**, *2*, 1955–1963.
[11] cF. T. F. O'Mahony, Y. H. Lee, C. Jellett, S. Dmitrov, D. T. Bryant, J. R. Durrant, B. C. O'Regan, M. Graetzel, M. K. Nazeeruddin, S. A. Haque, *J. Mater. Chem. A* **2015**, *3*, 7219–7223.
[12] A. Gomes, E. Fernandes, J. Lima, *J. Biochem. Biophys. Methods* **2005**, *65*, 45–80.
[13] H. J. Snaith, *J. Phys. Chem. Lett.* **2013**, *4*, 3623–3630.
[14] O. J. Walker, *Trans. Faraday. Soc.* **1935**, *31*, 1432–1438.
[15] T. Baikie, Y. Fang, J. M. Kadro, M. Schreyer, F. Wei, S. G. Mhaisalkar, M. Graetzel, T. J. White, *J. Mater. Chem. A* **2013**, *1*, 5628–5641.
[16] D. S. Bhachu, D. O. Scanlon, E. J. Saban, H. Bronstein, I. P. Parkin, C. J. Carmalt, R. G. Palgrave, *J. Mater. Chem. A* **2015**, *3*, 9071–9073.
[17] N. J. Jeon, J. H. Noh, Y. C. Kim, W. S. Yang, S. Ryul, S. I. Seok, *Nat. Mater.* **2014**, *13*, 897–903.

Received: April 6, 2015
Published online: May 26, 2015